LETTER

doi:10.1038/nature10545

Membrane protein sequestering by ionic protein–lipid interactions

Geert van den Bogaart[1], Karsten Meyenberg[2], H. Jelger Risselada[3], Hayder Amin[1], Katrin I. Willig[4], Barbara E. Hubrich[2], Markus Dier[1], Stefan W. Hell[4], Helmut Grubmüller[3], Ulf Diederichsen[2] & Reinhard Jahn[1]

Neuronal exocytosis is catalysed by the SNAP receptor protein syntaxin-1A[1], which is clustered in the plasma membrane at sites where synaptic vesicles undergo exocytosis[2,3]. However, how syntaxin-1A is sequestered is unknown. Here we show that syntaxin clustering is mediated by electrostatic interactions with the strongly anionic lipid phosphatidylinositol-4,5-bisphosphate (PIP2). Using super-resolution stimulated-emission depletion microscopy on the plasma membranes of PC12 cells, we found that PIP2 is the dominant inner-leaflet lipid in microdomains about 73 nanometres in size. This high accumulation of PIP2 was required for syntaxin-1A sequestering, as destruction of PIP2 by the phosphatase synaptojanin-1 reduced syntaxin-1A clustering. Furthermore, co-reconstitution of PIP2 and the carboxy-terminal part of syntaxin-1A in artificial giant unilamellar vesicles resulted in segregation of PIP2 and syntaxin-1A into distinct domains even when cholesterol was absent. Our results demonstrate that electrostatic protein–lipid interactions can result in the formation of microdomains independently of cholesterol or lipid phases.

Phosphoinositides are lipids that contain an inositol head group conjugated to one to three phosphate groups. With ~1% of total lipids in the inner leaflet of the plasma membrane[4], PIP2 is the most abundant phosphoinositide. Earlier studies identified PIP2 as a second messenger in the phospholipase-C signalling pathway. However, the list of cellular functions of PIP2 is rapidly growing, and PIP2 is also involved in membrane targeting, cytoskeletal attachment, endocytosis and exocytosis[4]. PIP2 interacts with many different proteins, through either unstructured basic residue-rich regions or more-structured domains[4,5].

Neuronal exocytosis requires the presence of PIP2 at the plasma membrane[2,6–8]. The amount of PIP2 at the plasma membrane determines the rate of vesicle priming, the size of the readily releasable pool and the rate of sustained exocytosis in stimulated cells[2,6,8]. This regulation is probably mediated by interactions of PIP2 with proteins involved in docking and fusion such as rabphilin, CAPS, synaptotagmin, SCAMP2 and Mint proteins[6,9]. In docking, PIP2 clusters may act as molecular 'beacons' that target synaptic vesicles to the fusion sites. Indeed, PIP2 is locally enriched at the sites of docked vesicles and co-localizes with at least 5–10% of the microdomains of syntaxin-1A[2,3,9] (Supplementary Fig. 1), the membrane-anchored target SNAP receptor of neuronal exocytosis[1].

The amount of PIP2 at the sites of membrane fusion in PC12 cells has been estimated at 3–6% PIP2 coverage of local cell surface area[9] (Supplementary Fig. 2). In these experiments, membrane sheets were specifically stained for PIP2 with the Pleckstrin homology domain of protein lipase C delta fused to green fluorescent protein[9] or citrine (a yellow fluorescent protein analogue[10]; $PH_{PLC\delta}$–citrine; Supplementary Figs 1 and 2), and the fluorescence of the punctuated PIP2 microdomains was quantified. However, this approach underestimates the fraction of PIP2 if the $PH_{PLC\delta}$ microdomains are smaller than the ~200-nm diffraction-limited resolution of conventional fluorescence microscopy[9]. To obtain a more accurate estimate, we re-analysed PC12 membrane sheets labelled with $PH_{PLC\delta}$–citrine or an antibody raised against PIP2 using super-resolution stimulated-emission depletion (STED) microscopy[11] (Fig. 1a–c). These experiments revealed that the clusters stained for PIP2 are much smaller than anticipated, with an average diameter of only 73 ± 42 nm (s.d.). Although this is an overestimate because it represents the microdomain size convolved with the resolution of the STED microscope (~60 nm), it is in good agreement with the size of the syntaxin-1A microdomains[12].

Using a microdomain size of 73 nm, we recalculated the surface density of PIP2 (Supplementary Methods). For this calculation, we first estimated the total amount of PIP2 in a microdomain when sampled at the diffraction-limited resolution of our epifluorescence

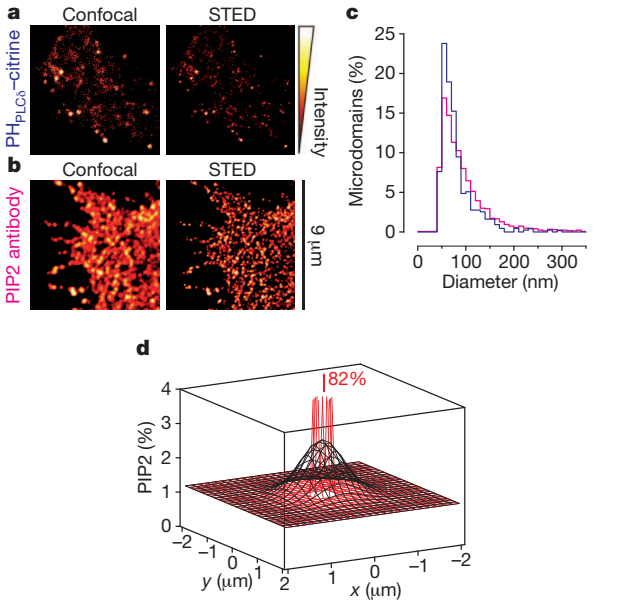

Figure 1 | PIP2 is the predominant inner-leaflet lipid in roughly 73-nm-sized microdomains. **a**, Confocal and corresponding nanoscale-resolution STED image of a $PH_{PLC\delta}$–citrine-stained membrane sheet of PC12 cells. Note the increase in resolution. **b**, Same as **a**, but now immunostained with a monoclonal PIP2 antibody and a secondary antibody labelled with Alexa Fluor 488. **c**, Size distribution of microdomains with $PH_{PLC\delta}$–citrine (blue; $n = 433$, 24 sheets, two independent preparations) and PIP2 antibody (pink; $n = 2{,}959$, 22 sheets, two independent preparations). The average diameter (full-width at half-maximum) was 73 ± 42 nm (s.d.) for microdomains with $PH_{PLC\delta}$–citrine and 87 ± 62 nm (s.d.) for microdomains with PIP2 antibody. **d**, Spatial distribution of PIP2. Black: the PIP2 distribution when sampled at too low diffraction-limited resolution (377 nm; Supplementary Fig. 2). Red: approximation of the PIP2 distribution in the ~73-nm microdomains. PIP2 was accumulated over ~82% of the total surface area. See Supplementary Methods for details.

[1]Department of Neurobiology, Max Planck Institute for Biophysical Chemistry, Am Faßberg 11, 37077 Göttingen, Germany. [2]Institute for Organic and Biomolecular Chemistry, Georg-August-University Göttingen, Tammannstraße 2, 37077 Göttingen, Germany. [3]Department of Theoretical and Computational Biophysics, Max Planck Institute for Biophysical Chemistry, Am Faßberg 11, 37077 Göttingen, Germany. [4]Department of Nanobiophotonics, Max Planck Institute for Biophysical Chemistry, Am Faßberg 11, 37077 Göttingen, Germany.

microscope (Fig. 1d, black mesh, and Supplementary Fig. 2). We then calculated the peak concentration when this amount of PIP2 was concentrated into 73-nm microdomains (Fig. 1d, red mesh). Here we assumed a Gaussian distribution of PIP2 in the microdomains. A peak surface coverage of 82% PIP2 was obtained (Fig. 1d). It must be kept in mind that at these high PIP2 concentrations, molecular crowding might hinder binding of $PH_{PLC\delta}$–citrine; that relatively small errors in microdomain size and microscope resolution result in a substantial error in the PIP2 coverage; and that $PH_{PLC\delta}$–citrine and antibody binding may alter PIP2 localization and is only indicative of PIP2 microdomains. Nevertheless, the PIP2 concentrations that we calculate are much higher than any previous estimate, and it seems safe to conclude that PIP2 is the dominant inner-leaflet lipid in the microdomains. The question then arises of by which molecular mechanism such high concentrations of PIP2 are achieved.

PIP2 has a net negative charge of −3 to −5 (ref. 4) and interacts with polybasic stretches of amino acids[4,5,13,14]. Proteins with such stretches can sequester PIP2 in amounts in excess even of monovalent anionic lipids, such as MARCKS, spermine and even pentalysine[5,14]. Similar to these proteins, syntaxin-1A also possesses a stretch of basic amino acids. These residues are adjacent to the transmembrane domain and are in contact with the head groups of the phospholipids[15,16] (Supplementary Fig. 3a). Indeed, it is well established that this conserved stretch with five positive residues (^{260}KARRKK^{265}) interacts with PIP2[9,15–17]. Removal of charge weakens this interaction (Supplementary Fig. 3b, c), but syntaxin-1A remains capable of fusing membranes even on removal of all five charges[9,16]. Because PIP2 colocalizes with at least a fraction of syntaxin-1A microdomains[2] (Supplementary Fig. 1), we speculated that their interaction might drive domain formation in a manner similar to that in various soluble lipid-binding proteins[5,14]. Two independent approaches were used to test this hypothesis: reconstitution in giant unilamellar vesicles[18] (GUVs) and hydrolysis of PIP2 in PC12 cells using a membrane-targeted variant of the PIP2 phosphatase synaptojanin-1[7].

Syntaxin-1A clustered in a non-raft way in neutral cholesterol–phosphatidylcholine membranes[17]. Here cholesterol clusters syntaxin-1A by competing for solvation by phosphatidylcholine. Indeed, a synthetic C-terminal peptide of syntaxin-1A (residues 257–288; 3 mol%; Fig. 2 and Supplementary Fig. 4a) clustered in domains in >50% of GUVs composed of 1,2-dioleoyl-*sn*-glycero-3-phosphatidylcholine (DOPC) with 20 mol% cholesterol. This peptide contained both the polybasic juxtamembrane linker and transmembrane region and was amino-terminally labelled with either rhodamine red or Atto 647N. Analysis of fluorescence showed a (1.6 ± 0.2)-fold (s.d.; $n = 18$) enrichment of syntaxin-$1A_{257–288}$ in these clusters, but this is an underestimate limited by the optics. Negatively charged PIP2 or 1,2-dioleoyl-*sn*-glycero-3-phosphatidylserine (DOPS) dispersed these clusters[17] (Fig. 2). Thus, although cholesterol competition might explain syntaxin-1A clusters that are not enriched in PIP2 (Supplementary Fig. 1), it cannot explain the high accumulation of PIP2 at the sites of docked vesicles. However, 1.5 mol% (total lipids) PIP2 also clustered syntaxin-1A in 1–10-μm domains in 1–5% of the GUVs (Fig. 2 and Supplementary Fig. 4b, c). These domains did not depend on cholesterol or DOPS. In these domains, PIP2 was (1.9 ± 0.2)-fold (s.d.; $n = 13$; Supplementary Fig. 5) enriched and syntaxin-$1A_{257–288}$ was (5.5 ± 1.4)-fold (s.d.; $n = 27$) enriched, calculated on the basis of fluorescence. Notably, no domains were observed without peptide or when the PIP2 concentration exceeded 5 mol%. Divalent cations can act as bridges between two adjacent lipids and induce aggregation of PIP2 into clusters[19–21], but even 1 mM Ca^{2+} was not sufficient to attract syntaxin-1A away from the microdomains. Domains were present both for synthetic dioleoyl-PIP2 and for PIP2 extracted from pig brain (Supplementary Fig. 4b). Thus, syntaxin-1A can be clustered in the membrane by both cholesterol and PIP2.

These cholesterol- and PIP2-mediated clusters both differ from lipid 'rafts'. They also differ from each other. First, PIP2 domains are always

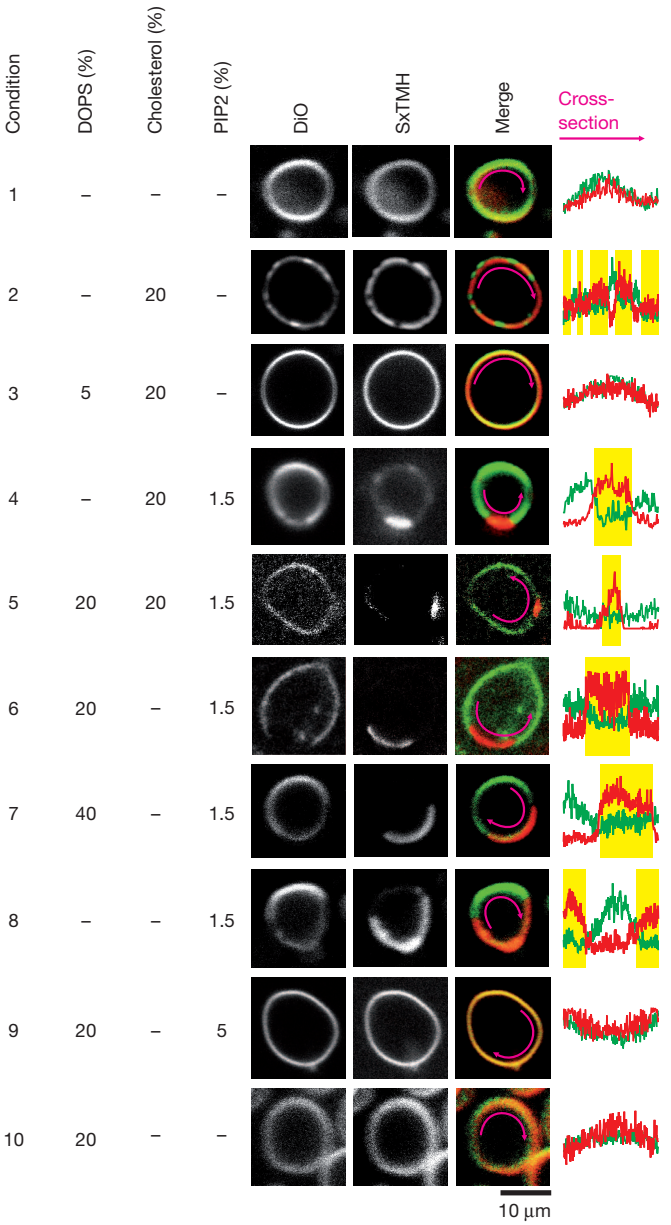

Figure 2 | Confocal microscopy of syntaxin-1A domains in artificial membranes. Syntaxin-$1A_{257–288}$ (SxTMH; red) labelled with Atto 647N was reconstituted in GUVs. The membranes were composed of DOPC with 1.5 mol% of the fluorescent lipid analogue 3,3′-dioctadecyloxacarbocyanine (DiO; green) and the percentages DOPS, cholesterol and PIP2 indicated in the figure. In the absence of anionic phospholipids, 20% cholesterol clustered syntaxin-1A in many small clusters (condition 2), as predicted in ref. 17. Inclusion of >5% anionic DOPS dispersed these clusters (condition 3). PIP2 (1.5%) partitioned SxTMH in 1–10-μm-sized domains regardless of cholesterol or DOPS (conditions 4–8). These clusters were no longer observed with 5% PIP2 (condition 9). The pink arrows show the part of the membrane used for cross-sections. Yellow bars indicate the positions of the domains. More data are presented in Supplementary Figs 4–9.

round and only one or two form per vesicle, whereas cholesterol generally (but not always) induces many small domains (Supplementary Fig. 4). Second, fluorescence recovery after photobleaching showed that syntaxin-1A remained mobile in the PIP2 domains and that syntaxin-1A was essentially immobile in the cholesterol-dependent clusters (Supplementary Fig. 6). Syntaxin-1A thus diffuses in the PIP2 domains and forms large circular domains to minimize boundary energy[21]. Third, 6-dodecanoyl-2-dimethylaminonaphthalene[22] (laurdan) showed that the PIP2 domains were highly hydrated, whereas the

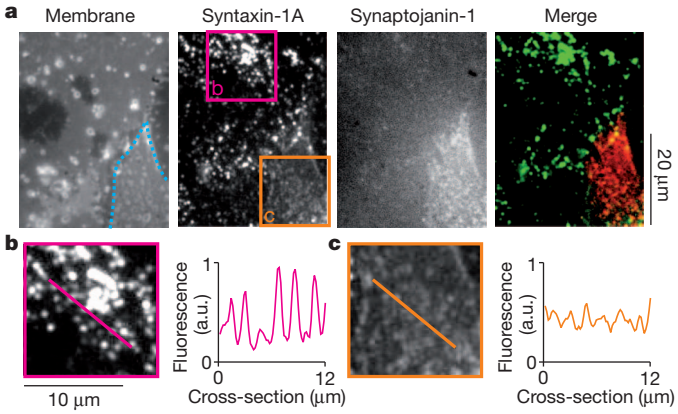

Figure 3 | Removal of PIP2 reduces syntaxin-1A clustering in PC12 cells. **a**, Membrane sheets of PC12 cells stained with 1-(4-trimethylammoniumphenyl)-6-phenyl-1,3,5-hexatriene[12,24] (TMA-DPH). Immunostaining with a monoclonal antibody raised against syntaxin-1A and a secondary antibody labelled with DyLight649 showed that endogenous syntaxin-1A clustered in microdomains (region b; pink)[2,3,9,12,24]. Overexpressing the red-fluorescent-protein-tagged and membrane-targeted catalytic region of synaptojanin-1[7] (residues 498–901; cell outlined in blue) reduced this syntaxin-1A clustering 3.7-fold (region c; orange; Supplementary Fig. 13). Synaptojanin-1 is the 5-phosphatase of PIP2 and overexpression of the construct completely removes PIP2 from the membrane (Supplementary Fig. 12). **b**, **c**, Magnifications of regions b (**b**) and c (**c**). Cross-sections along the indicated cuts indicate the clustering. a.u., arbitrary units.

cholesterol domains were much more densely packed (Supplementary Fig. 7). Fourth, phase contrast microscopy showed a thickening of the cholesterol-dependent clusters but not of the PIP2-domains (Supplementary Fig. 8). Thus, even though no saturated lipids are present, the cholesterol-dependent domains have behaviour that resembles the liquid ordered phase. In contrast, the PIP2 domains seem much more disordered and resemble the liquid disordered phase. Ca^{2+} demixing of polyanionic amphiphiles showed that electrostatic interactions can indeed lead to liquid-like domains[21].

The transmembrane helix of syntaxin-1A has been reported to homodimerize. However, introducing the Met267Ala, Cys271Ala and Ile279Ala mutations that prevent homodimerization of the syntaxin-1A peptides[23] did not prevent cholesterol- or PIP2-mediated clustering (Supplementary Fig. 9). By contrast, no PIP2 domains were observed when two charges (Lys264Ala and Lys265Ala) from the polybasic linker were removed, but cholesterol-dependent clusters were still observed (Supplementary Fig. 5). Overexpression of the C-terminal part of syntaxin-1A fused to green fluorescent protein[24] in PC12 cells also showed 4–8-fold loss of clustering of the Lys264Ala Lys265Ala mutant (Supplementary Figs 10 and 11). These data show that electrostatic interactions between PIP2 and the juxtamembrane helix of syntaxin-1A are sufficient for domain formation.

We then set out to investigate to what extent PIP2 is required for syntaxin-1A clustering in PC12 cells. For this purpose, we expressed a red-fluorescent-protein-tagged construct containing the phosphatase domain of synaptojanin-1 fused to a CAAX box, resulting in its targeting to the plasma membrane[7]. Synaptojanin-1 is a polyphosphoinositide 5-phosphatase, and the expression of the construct completely removed PIP2 from the plasma membrane[6,7] (Supplementary Fig. 12). Notably, synaptojanin-1 expression reduced 3.7-fold the punctuate distribution of endogenous syntaxin-1A (Fig. 3 and Supplementary Fig. 13). Thus, this provides evidence that PIP2 is indeed required for at least part of syntaxin-1A microdomain formation.

We performed molecular dynamics simulations to gain insight into the precise conformation of the PIP2/syntaxin-1A microdomains. In these coarse-grained simulations, several atoms were represented by one simulation bead[25,26] (Supplementary Fig. 14). This allowed for simulations of relatively large lipid bilayers comprising ~2,500 copies of DOPC and DOPS in a 4:1 molar ratio and 40–64 copies of syntaxin-$1A_{257–288}$ and PIP2. In a simulation time of 10 μs, up to ten copies of syntaxin-$1A_{257–288}$ clustered with PIP2 into microdomains (Supplementary Fig. 15). Equal amounts of PIP2 and syntaxin-1A were present in the bulk phase of those domains, whereas more PIP2 and DOPS associated transiently to the periphery. We used this information to construct a domain with 64 copies of syntaxin-1A (Fig. 4 and Supplementary Movie 1), which is comparable to the syntaxin-1A content in the microdomains in PC12 cells[12]. These domains were stable over a simulation time of 6 μs and contained <10% residual DOPC or DOPS. We conclude that syntaxin-1A and PIP2 can form dynamic, amorphous networks with PIP2 acting as a 'charge bridge' spanning the distance between the various syntaxin-1A molecules (Fig. 4c).

Our findings show that electrostatic interactions between the membrane lipid PIP2 and the SNAP receptor syntaxin-1A suffice to induce membrane sequestering and microdomain formation without the need for high local PIP2 production or a (complex) 'molecular fence' restricting PIP2 and protein diffusion[27]. This does not exclude an additional role for protein–protein interactions between either

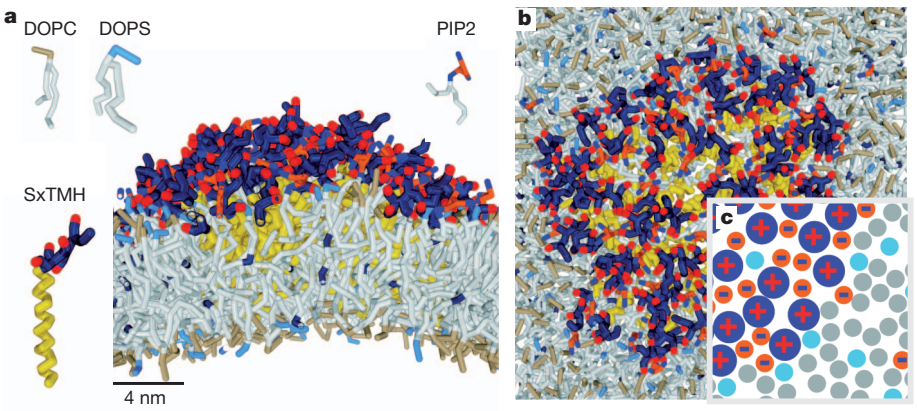

Figure 4 | Simulations of the dynamic and amorphous PIP2/syntaxin-1A microdomains. **a**, **b**, Side view (**a**) and top view (**b**) of a coarse-grained molecular dynamics simulation. Sixty-four copies of syntaxin-$1A_{257–288}$ (SxTMH) and 64 copies of PIP2 were incorporated in a bilayer composed of DOPC and DOPS in a 4:1 molar ratio. PIP2 was present only in the membrane leaflet facing the N-terminus of syntaxin-$1A_{257–288}$. Simulations were performed with 150 mM NaCl. See Supplementary Methods for details. White, lipid alkyl chain; cyan, DOPS head group; grey, DOPC head group; yellow, syntaxin-$1A_{257–288}$ transmembrane region (residues 266–288); blue–red, polybasic linker region (residues 257–265; charges in red); orange–blue, anionic PIP2 head group (charges in blue). The domains were stable over a simulation time of 6 μs (Supplementary Movie 1). **c**, Simplified scheme of the cluster.

transmembrane helices or soluble domains. In fact, these seem essential for segregation of proteins with similar structures and sizes, such as syntaxin-1A and syntaxin-4[12,24] (both have polybasic regions and cluster separately). The mutual enrichment of syntaxin-1A and PIP2 at the fusion sites by electrostatic interactions has clear advantages. First, accumulation of syntaxin-1A may facilitate SNAP receptor interactions and thereby increase the membrane fusion efficiency[3,28]. Second, the lipid environment modulates the energetic requirements for fusion[13,16]. Third, both PIP2 and syntaxin-1A function as molecular docking sites and facilitate assembly of the complete fusion machinery[1,2,6–9]. Our findings that electrostatic protein–lipid interactions are sufficient for membrane sequestering indicate that such interactions constitute a mechanism for the formation of protein microdomains in the membrane that is clearly distinct from protein partitioning by means of the well-established lipid phases[18,29].

METHODS SUMMARY

$PH_{PLC\delta}$–citrine was expressed in *Escherichia coli* and purified using His-tag affinity purification. PC12 cells were maintained and propagated as described in refs 3, 24. PC12 cells were transfected using Lipofectamine LTX (Invitrogen). Membrane sheets were prepared by rupturing the cells with probe sonication as described in ref. 24, and immunostaining[24] and microscopy[11,24] were performed as described in the corresponding references. The peptides were synthesized by microwave-assisted Fmoc solid-phase synthesis. Peptides were mixed with lipids in organic solvent and GUVs were formed by the drying rehydration procedure. The molecular dynamics simulations were performed with the GROMACS simulation package and the MARTINI coarse-grained model[25,26]. See Supplementary Methods for details.

Received 24 May; accepted 7 September 2011.
Published online 23 October 2011.

1. Jahn, R. & Scheller, R. H. SNAREs – engines for membrane fusion. *Nature Rev. Mol. Cell Biol.* **7,** 631–643 (2006).
2. Aoyagi, K. *et al.* The activation of exocytotic sites by the formation of phosphatidylinositol 4,5-bisphosphate microdomains at syntaxin clusters. *J. Biol. Chem.* **280,** 17346–17352 (2005).
3. Lang, T. *et al.* SNAREs are concentrated in cholesterol-dependent clusters that define docking and fusion sites for exocytosis. *EMBO J.* **20,** 2202–2213 (2001).
4. McLaughlin, S., Wang, J., Gambhir, A. & Murray, D. PIP(2) and proteins: interactions, organization, and information flow. *Annu. Rev. Biophys. Biomol. Struct.* **31,** 151–175 (2002).
5. McLaughlin, S. & Murray, D. Plasma membrane phosphoinositide organization by protein electrostatics. *Nature* **438,** 605–611 (2005).
6. Wen, P. J., Osborne, S. L. & Meunier, F. A. Dynamic control of neuroexocytosis by phosphoinositides in health and disease. *Prog. Lipid Res.* **50,** 52–61 (2011).
7. Milosevic, I. *et al.* Plasmalemmal phosphatidylinositol-4,5-bisphosphate level regulates the releasable vesicle pool size in chromaffin cells. *J. Neurosci.* **25,** 2557–2565 (2005).
8. Hay, J. C. & Martin, T. F. Phosphatidylinositol transfer protein required for ATP-dependent priming of Ca^{2+}-activated secretion. *Nature* **366,** 572–575 (1993).
9. James, D. J., Khodthong, C., Kowalchyk, J. A. & Martin, T. F. Phosphatidylinositol 4,5-bisphosphate regulates SNARE-dependent membrane fusion. *J. Cell Biol.* **182,** 355–366 (2008).
10. Griesbeck, O., Baird, G. S., Campbell, R. E., Zacharias, D. A. & Tsien, R. Y. Reducing the environmental sensitivity of yellow fluorescent protein. Mechanism and applications. *J. Biol. Chem.* **276,** 29188–29194 (2001).
11. Hell, S. W. & Wichmann, J. Breaking the diffraction resolution limit by stimulated emission: stimulated-emission-depletion fluorescence microscopy. *Opt. Lett.* **19,** 780–782 (1994).
12. Sieber, J. J. *et al.* Anatomy and dynamics of a supramolecular membrane protein cluster. *Science* **317,** 1072–1076 (2007).
13. Williams, D., Vicôgne, J., Zaitseva, I., McLaughlin, S. & Pessin, J. E. Evidence that electrostatic interactions between vesicle-associated membrane protein 2 and acidic phospholipids may modulate the fusion of transport vesicles with the plasma membrane. *Mol. Biol. Cell* **20,** 4910–4919 (2009).
14. Denisov, G., Wanaski, S., Luan, P., Glaser, M. & McLaughlin, S. Binding of basic peptides to membranes produces lateral domains enriched in the acidic lipids phosphatidylserine and phosphatidylinositol 4,5-bisphosphate: an electrostatic model and experimental results. *Biophys. J.* **74,** 731–744 (1998).
15. Kweon, D. H., Kim, C. S. & Shin, Y. K. The membrane-dipped neuronal SNARE complex: a site-directed spin labeling electron paramagnetic resonance study. *Biochemistry* **41,** 9264–9268 (2002).
16. Lam, A. D., Tryoen-Toth, P., Tsai, B., Vitale, N. & Stuenkel, E. L. SNARE-catalyzed fusion events are regulated by syntaxin1A-lipid interactions. *Mol. Biol. Cell* **19,** 485–497 (2008).
17. Murray, D. H. & Tamm, L. K. Clustering of syntaxin-1A in model membranes is modulated by phosphatidylinositol 4,5-bisphosphate and cholesterol. *Biochemistry* **48,** 4617–4625 (2009).
18. Bacia, K., Schuette, C. G., Kahya, N., Jahn, R. & Schwille, P. SNAREs prefer liquid-disordered over ''raft'' (liquid-ordered) domains when reconstituted into giant unilamellar vesicles. *J. Biol. Chem.* **279,** 37951–37955 (2004).
19. Carvalho, K., Ramos, L., Roy, C. & Picart, C. Giant unilamellar vesicles containing phosphatidylinositol(4,5)bisphosphate: characterization and functionality. *Biophys. J.* **95,** 4348–4360 (2008).
20. Levental, I. *et al.* Calcium-dependent lateral organization in phosphatidylinositol 4,5-bisphosphate (PIP2)- and cholesterol-containing monolayers. *Biochemistry* **48,** 8241–8248 (2009).
21. Christian, D. A. *et al.* Spotted vesicles, striped micelles and Janus assemblies induced by ligand binding. *Nature Mater.* **8,** 843–849 (2009).
22. Kaiser, H. J. *et al.* Order of lipid phases in model and plasma membranes. *Proc. Natl Acad. Sci. USA* **106,** 16645–16650 (2009).
23. Laage, R., Rohde, J., Brosig, B. & Langosch, D. A conserved membrane-spanning amino acid motif drives homomeric and supports heteromeric assembly of presynaptic SNARE proteins. *J. Biol. Chem.* **275,** 17481–17487 (2000).
24. Sieber, J. J., Willig, K. I., Heintzmann, R., Hell, S. W. & Lang, T. The SNARE motif is essential for the formation of syntaxin clusters in the plasma membrane. *Biophys. J.* **90,** 2843–2851 (2006).
25. Marrink, S. J., Risselada, H. J., Yefimov, S., Tieleman, D. P. & de Vries, A. H. The MARTINI forcefield: coarse grained model for biomolecular simulations. *J. Phys. Chem. B* **111,** 7812–7824 (2007).
26. Yesylevskyy, S., Schafer, L. V., Sengupta, D. & Marrink, S. J. Polarizable water model for the coarse-grained Martini force field. *PLoS Comp. Biol.* **6,** e1000810 (2010).
27. Fujiwara, T., Ritchie, K., Murakoshi, H., Jacobson, K. & Kusumi, A. Phospholipids undergo hop diffusion in compartmentalized cell membrane. *J. Cell Biol.* **157,** 1071–1082 (2002).
28. van den Bogaart, G. & Jahn, R. Counting the SNAREs needed for membrane fusion. *J. Mol. Cell Biol.* **3,** 204–205 (2011).
29. Simons, K. & Ikonen, E. Functional rafts in cell membranes. *Nature* **387,** 569–572 (1997).

Supplementary Information is linked to the online version of the paper at www.nature.com/nature.

Acknowledgements We thank M. Holt, G. Bunt, F. S. Wouters and C. Eggeling for advice, and V. Haucke and S. Joo for the red-fluorescent-protein-tagged synaptojanin-1 construct. G.v.d.B. is financed by the Human Frontier Science Program. This work was supported by the US National Institutes of Health (P01 GM072694, to R.J.) and the Deutsche Forschungsgemeinschaft (SFB803, to K.M., H.J.R., U.D., H.G. and R.J.).

Author Contributions G.v.d.B. and R.J. designed the experiments and wrote the paper. K.M., B.E.H. and U.D. synthesized the peptides. H.J.R. and H.G. performed the simulations. K.I.W. and S.W.H performed the STED microscopy. H.A. and M.D. contributed to the protein purification, immunofluorescence and microscopy. G.v.d.B. performed all other experiments. All authors contributed to writing the manuscript.

Author Information Reprints and permissions information is available at www.nature.com/reprints. The authors declare no competing financial interests. Readers are welcome to comment on the online version of this article at www.nature.com/nature. Correspondence and requests for materials should be addressed to R.J. (r.jahn@gwdg.de).